Version of Record: https://www.sciencedirect.com/science/article/pii/S0032386122004591
Manuscript_3763615bffbde654f1dc84c0c1747e8a

Reprocessable Polyhydroxyurethane Networks Reinforced with Reactive Polyhedral Oligomeric Silsesquioxanes (POSS) and Exhibiting Excellent Elevated Temperature Creep Resistance

Sumeng Hu,[a] Xi Chen,[a] Mohammed A. Bin Rusayyis,[b] Nathan S. Purwanto,[b] and John M. Torkelson[a,b,*]

[a]Department of Chemical and Biological Engineering, Northwestern University, 2145 Sheridan Road, Evanston, IL 60208 USA

[b]Department of Materials Science and Engineering, Northwestern University, 2145 Sheridan Road, Evanston, IL 60208 USA

*Corresponding author (j-torkelson@northwestern.edu)

Abstract. The rapid development of covalent adaptable networks or vitrimers shows promise for addressing the long-standing recycling issues associated with conventional, permanently cross-linked thermosets. At the same time, it is important to demonstrate that properties of reprocessable polymer networks can be optimized to meet the ongoing demand for high-performance materials. We have fabricated reprocessable polyhydroxyurethane (PHU) network composites reinforced with reactive polyhedral oligomeric silsesquioxane (POSS). With functionalized POSS serving as a fraction of the cross-linkers, the PHU–POSS network nanocomposites exhibit significantly enhanced storage modulus at the rubbery plateau region relative to the neat PHU network. With up to 10 wt% POSS loading, these network composites can undergo melt-state reprocessing at 140 °C with 100% property recovery associated with cross-link density. We also show that hydroxyurethane dynamic chemistry leads to excellent creep resistance at elevated temperature up to 90 °C and is unaffected by reactive incorporation of POSS. This study demonstrates the effectiveness of POSS as nanofillers for designing high-performance, organic−inorganic dynamic PHU networks with excellent reprocessability.

1. Introduction

Thermosets have many advantages over thermoplastic materials including improved heat stability, solvent resistance, and enhanced physical properties because of their permanent network structures. However, the proper disposition of end-of-use thermosets remains a key challenge because the permanent cross-links that make these materials strong and useful prevent them from being melt-reprocessed or reshaped. In recent years, covalent adaptable networks (CANs) [1,2], also called dynamic covalent polymer networks (DCPNs) [3], have been developed to overcome the recyclability challenges associated with conventional thermosets. CANs contain a sufficient number of dynamic linkages to allow the materials to undergo network reconfiguration and thus to achieve recyclability under appropriate conditions [1]. Since the landmark study by Wudl and coworkers on a thermally re-mendable network designed with the Diels–Alder (DA) reaction [4], there has been considerable progress in developing CANs with numerous dynamic chemistries. These include dissociative chemistries such as hindered urea exchange [5–8], alkoxyamine chemistry [9–11], and bis(hindered amino) disulfide chemistry [12,13], and associative chemistries such as transesterification [14–17], boronic ester interchange [18–20], and transamination of vinylogous urethanes [21,22], among others [23–26]. CANs based on associative dynamic chemistries are often called vitrimers [14]. Some CANs have dual dynamic chemistries, e.g., polyhydroxyurethanes undergo associative transcarbamoylation and dissociative reversible cyclic carbonate aminolysis [27], and polythiourethanes undergo associative exchange reactions with free thiols and dissociative reversion to isocyanates and thiols [28,29]. The rapid development of CANs has bridged the gap between thermoplastics and thermosets [30–32] and shown promise for addressing the long-standing issue associated with the irreversible buildup of thermoset wastes. Reviews on the topic of sustainable, recyclable CANs, DCPNs, and vitrimers include refs. 31–39.

Fabrication of polymer nanocomposites by nanofiller incorporation is a common strategy to enhance the properties of polymeric materials [40–46]. The performance of nanocomposites is highly dependent on filler dispersion state and interfacial interactions between fillers and the

matrix [47–50]. Covalent modification of the filler surface for compatibilized polymer−filler interfaces is an effective method to achieve both high levels of filler dispersion and strong interfacial adhesion [49,51]. However, if CANs are used as the matrix, the restricted chain mobility induced by the improved adhesion of polymer chains onto the filler surface can impede topological rearrangement which is essential for relaxation-related properties such as self-healing ability and reprocessability [52]. Under such circumstances, surface-modified nanofillers with relatively small surface-to-volume ratios are desirable to balance the stress relaxation and mechanical property enhancement of dynamic network composites.

Polyhedral oligomeric silsesquioxanes (POSS) comprise cage-like organosilicon core $(SiO_{1.5})_n$ and external functional groups attached to each silicon atom [53–55]. Because the average POSS core diameter is only ~0.5 nm, POSS are considered to be the smallest possible particles of silica [55]. POSS are important building blocks to obtain organic–inorganic nanocomposites with enhanced properties because the reactive functional groups attached to the core provide a unique advantage for POSS molecules to be covalently bonded to the matrix and thus prevent filler aggregation. Several studies have applied functionalized POSS as reinforcing fillers to fabricate dynamic network composites. Xu et al. reported a tough, thermally mendable POSS nanocomposite synthesized from bismaleimide and octafunctional furan-terminated POSS via the DA reaction [55]. Because of the thermally reversible nature of the DA reaction, upon being cracked, the nanocomposite self-healed at appropriate temperatures. Zhou et al. [56] developed a mechanically strong, disulfide-based self-healable network composite by oxidative coupling of small-molecule thiols and octathiol-POSS. Although the composite relaxed stress more slowly than the matrix at lower temperatures, the difference in relaxation rate was lessened above 140 °C. As a result, the composite could be fully healed at higher temperatures or with longer healing time. Yang et al. [57] prepared a series of epoxy-POSS dynamic network composites by reacting dodecanedioic acid with a mixture of difunctional epoxy and octafunctional glycidyl ether-terminated POSS. The composites exhibited improved tensile strength with increasing POSS loading. With the help of the efficient transesterification

exchange reaction, the composites could be reprocessed with little degradation in mechanical properties. Related studies using functionalized POSS in developing dynamic covalent network composites have been done by Hajiali et al. [58] and Shen et al. [59]. These studies highlight the advantages and effectiveness of POSS for fabricating high-performance dynamic covalent network composites.

Polyhydroxyurethane (PHU) is synthesized by aminolysis of cyclic carbonates and is an environmentally friendly alternative to conventional isocyanate-based polyurethane (PU) [60–69]. In recent years, a number of studies have explored the inherent dynamic nature of cross-linked PHU and its effectiveness in developing CANs [27,70–72]. In 2015, Fortman et al. [70] reported that PHU networks derived from six-membered cyclic carbonates and amines can relax stress and be reprocessed at elevated temperatures. Their study showed the promise of cross-linked PHUs as a new class of reprocessable networks. In 2017, Torkelson and coworkers discovered that with appropriate catalysis, PHU networks derived from five-membered cyclic carbonates and amines can be reprocessed multiple times with 100% recovery of cross-link density [27]. Such reprocessability was also retained in some biobased PHU networks [71]. Torkelson and coworkers also developed reprocessable PHU network nanocomposites reinforced with silica nanoparticles with different surface functionalities [72]. When silica nanoparticles with surface hydroxyl and amine functional groups that can participate in dynamic chemistries with the matrix were used as fillers, reprocessing led to losses in cross-link density. Even when using superhydrophobic silica nanoparticles with surface hydroxyl groups mostly absent, the nanocomposite exhibited a ~10% loss in cross-link density relative to the as-synthesized material after the third reprocessing cycle due to the incomplete elimination of surface hydroxyl groups. These results indicate that an effective nanofiller species is still needed for the development of mechanically strong dynamic PHU network composites with excellent reprocessability.

A few studies have explored the use of POSS as reinforcing fillers to prepare PHU nanocomposites. Blattmann and Mülhaupt reported the preparation of organic–inorganic hybrid PHU thermosets using multifunctional POSS cyclic carbonates [73]. Zhao et al. investigated the

use of well-defined difunctional POSS macromers to synthesize physically cross-linked thermoplastic PHUs [74]. However, neither study focused on the influence of reactive POSS incorporation on the reprocessability of dynamic covalent PHU networks. Very recently, Liu et al. [75] synthesized PHUs using reactive trifunctional POSS cyclic carbonates as nanofiller, which led to nanocomposites with 20–40 nm POSS aggregates even at only 5 wt% POSS content. Compared with the original samples, the samples reprocessed by hot pressing exhibited decreases in tensile properties, which was attributed to the decrease in dynamic bond density after POSS incorporation and the restriction on segmental motion caused by POSS aggregation. Here, we have developed dynamic PHU network nanocomposites and investigated the effect of covalent incorporation of multifunctional POSS (with eight to twelve functional groups) on thermomechanical properties, reprocessability, and stress relaxation of dynamic PHU networks. As shown in Fig. 1, the PHU–POSS composites are synthesized by reacting difunctional amine JEFFAMINE D-400 with tris(4-hydroxyphenyl)methane tricarbonate (THPMTC) and POSS-cyclic carbonate (POSS-CC). With increasing POSS loading, the composites exhibit improved thermal stability and enhanced rubbery plateau modulus. More importantly from a sustainability standpoint, the as-synthesized composites containing up to 10 wt% multifunctional POSS can undergo multiple reprocessing cycles with 100% property recovery associated with cross-link density. This study highlights the potential of POSS for fabricating fully recyclable, cross-linked PU-like materials made by non-isocyanate chemistry.

2. Experimental

2.1. Materials. Tris(4-hydroxyphenyl)methane triglycidyl ether (THPMTE), tetrabutylammonium iodide (TBAI, reagent grade, 98%), *N*,*N*-dimethylacetamide (DMAc, anhydrous, 99.8%), dimethylformamide (DMF, anhydrous, 99.8%), 4-(dimethylamino)pyridine (DMAP), and dimethyl sulfoxide-d6 (DMSO-d6, 99.9 atom% D) were purchased from Sigma-Aldrich and used as received. Methylene chloride (DCM) was purchased from Fisher Chemical and used as received. JEFFAMINE D-400 (D400) was supplied by HUNTSMAN and was kept

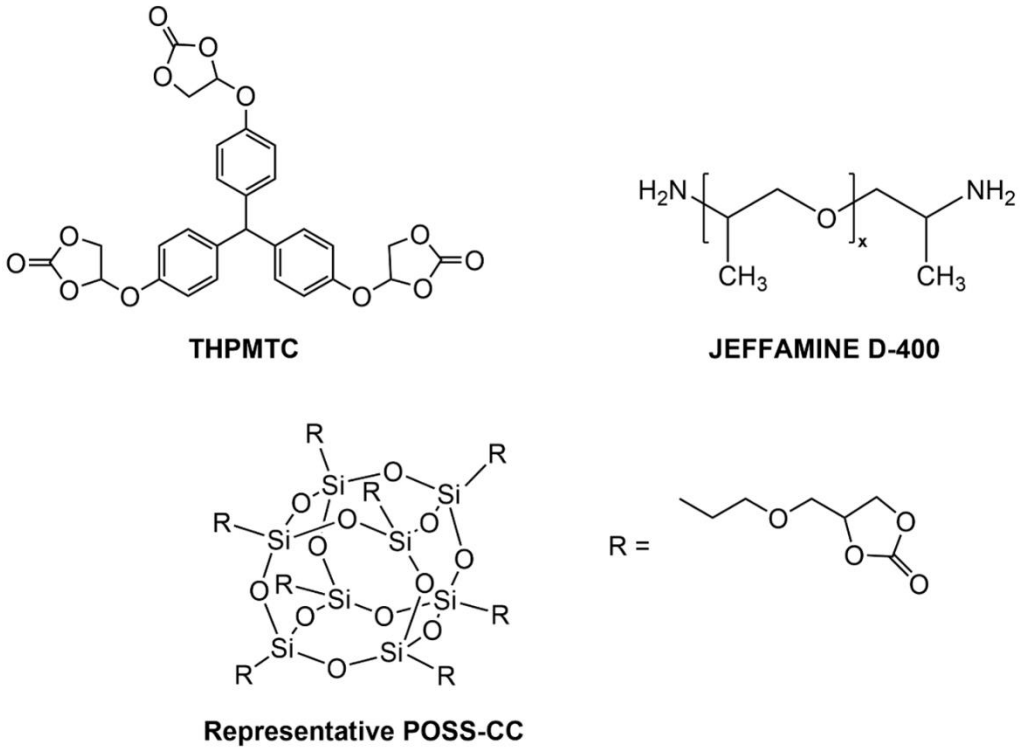

Fig. 1. Structures of the compounds used for PHU−POSS synthesis.

on activated molecular sieve before use. POSS glycidyl ether (EP0409), consisting of a mixture of POSS glycidyl ethers with different cage sizes, was purchased from Hybrid Plastics and used as received.

2.2. Synthesis of POSS-CC and THPMTC. POSS-CC was synthesized by CO_2 fixation of EP0409 in the presence of TBAI. EP0409 (13.00 g, containing 77.84 mmol of epoxy groups) and TBAI (0.58 g, 1.56 mmol, 2 mol% relative to epoxy groups) were placed in a 50-mL test tube along with 20 mL DMAc that helped to dissolve TBAI. The test tube was placed in an oil bath at 80 °C, and CO_2 gas was bubbled through the mixture until complete conversion of epoxy groups to cyclic carbonate groups was achieved (~5 days). The reaction progress was periodically checked by ^{1}H NMR spectroscopy by observing the disappearance of proton signals associated with the epoxy moiety. Upon completion, the mixture became a highly viscous liquid. TBAI was removed by dissolving the mixture with acetone and precipitating with distilled water for seven times. The purified product was dried in an 80 °C vacuum oven for 48 h. The carbonate content

in POSS-CC was determined via ^{1}H NMR spectroscopy using DMSO as solvent and 1,2,4,5-tetrachlorobenzene as an internal reference. The following equation was used to calculate the moles of carbonate groups per gram of POSS-CC:

$$\text{carbonate content } [\frac{\text{mol}}{\text{g}}] = \frac{I_{\text{cc}} \times n_{\text{ref}}}{\frac{I_{\text{ref}}}{2} \times m_{\text{POSS-CC}}} \quad (1)$$

where I_{cc} is the intensity of the peak associated with one of the three protons on cyclic carbonate in POSS-CC (~4.89 ppm), n_{ref} is the molar amount of 1,2,4,5-tetrachlorobenzene in the ^{1}H NMR sample, I_{ref} is the peak intensity associated with the two protons on 1,2,4,5-tetrachlorobenzene (~8.07 ppm), and $m_{POSS-CC}$ is the weight of POSS-CC in the sample.

THPMTC was synthesized following a similar procedure that used to prepare POSS-CC. In a typical synthesis of THPMTC, THPMTE (20.00 g, 43.43 mmol) and TBAI (1.60 g, 4.34 mmol) were placed in a test tube along with 20 mL DMAc that helped to dilute the reaction mixture. The test tube was heated in an oil bath at 80 °C. CO_2 gas was continuously bubbled through the mixture until full conversion of epoxy groups into cyclic carbonate groups was confirmed by ^{1}H NMR (Fig. S3). After the reaction was completed, TBAI was removed by dissolving the product with acetone and washing with water for seven times. The final product was completely dried in a vacuum oven at 80 °C for 48 h.

2.3. Synthesis of neat PHU network and PHU–POSS composites. PHU–POSS composites were prepared by reacting the mixture of THPMTC and POSS-CC with difunctional amine D400 under DMAP catalysis. In a typical synthesis of PHU−POSS composite containing 10 wt% POSS-CC, 0.878 g THPMTC (containing 4.45 mmol cyclic carbonate), 0.238 g POSS-CC (containing 1.42 mmol cyclic carbonate), and 71.6 mg DMAP (0.587 mmol) was dissolved with 1.5 mL DMF in a 20-mL scintillation vial. After complete solubilization, 1.26 g D400 (containing 5.87 mmol of primary amine groups) was added into the vial dropwise. The mixture was reacted at 85 °C for 20 h in an oil bath. Then, dry nitrogen gas was flowed through the vial for 4 h to evaporate some DMF before the gelled product was cut into small pieces and further dried in a nitrogen-purged 85 °C vacuum oven for 48 h. Neat PHU networks were synthesized in

a similar manner without the addition of POSS-CC.

2.4. Reprocessing procedure for neat PHU network and PHU–POSS nanocomposites. Reprocessing of neat PHU networks and PHU−POSS composites was performed using a PHI press (model 0230C-X1). The dried, as-synthesized materials in the form of small pieces were pressed into ~1-mm-thick sheets at 140 °C with a 7-ton ram force (generating a pressure of ~11 MPa). After the first reprocessing cycle, the uniform, flat sheets were considered as the 1st molded samples. The 1st molded samples were further cut into small pieces and pressed again to give another batch of flat sheets, which are considered as the 2nd molded samples. A 2.0 h reprocessing time was used for the neat PHU network and PHU–POSS composites containing 5 wt% POSS-CC (PHU-POSS-5). For PHU–POSS composites containing 10 wt% POSS-CC (PHU-POSS-10), the reprocessing time from the original materials to the 1st molded materials was 2.5 h, and that from the 1st molded materials to the 2nd molded materials was 1.5 h.

2.5. Equilibrium swelling experiments. Swelling experiments were conducted at room temperature using DCM as solvent. Small network pieces were placed in ~20 ml DCM in a glass vial and swollen for 3 days to equilibrium. Swollen samples were immediately weighed after removing the remaining solvent on the network surface. The networks were then dried at 80 °C in a vacuum oven for 3 days and weighed afterwards. The gel fraction is calculated as m_{dry}/m_0, and the swelling ratio is calculated as $(m_{sw} - m_{dry})/m_{dry}$, where m_0, m_{sw}, and m_{dry} are the masses of the original samples, swollen samples, and dried samples, respectively.

2.6. Characterization. Attenuated total reflectance-Fourier transform infrared (ATR-FTIR) spectroscopy was performed using a Bruker Tensor 37 MiD IR FTIR spectrophotometer equipped with a diamond/ZnSe ATR attachment. Thirty-two scans were collected at room temperature over the 4000 to 800 cm^{-1} range with a 2 cm^{-1} resolution. ^1H NMR spectroscopy was performed at room temperature using a Bruker Avance III 500 MHz NMR spectrometer with a direct cryoprobe.

Dynamic mechanical analysis (DMA) was performed using a TA Instruments RSA G2 DMA. Rectangular samples measuring ~0.9 mm in thickness and ~3 mm in width were mounted

on the fixture and underwent temperature ramps from −10 °C to 80 °C at a 3 °C/min heating rate. The tensile storage modulus (E'), tensile loss modulus (E''), and tan δ (E''/E') were measured in tension mode at 1 Hz frequency and 0.03% strain.

Stress relaxation experiments were performed using a TA Instruments RSA G2 DMA. Rectangular samples measuring ~0.9 mm in thickness and ~3 mm in width were mounted on the fixture and allowed to equilibrate at the desired temperature for 15 min before being subjected to an instantaneous strain of 5%. The stress relaxation modulus at 5% strain was recorded until it decayed to ~20% of its initial value. Stress relaxation experiments were carried out at 140–170 °C at 10 °C increments.

Shear creep experiments at 3.0 kPa stress were performed on 1st molded, ~2 mm-thick disk samples using an Anton-Paar MCR 302 rheometer with 25-mm parallel-plate fixtures. Samples were equilibrated at the test temperature for 10 min before starting the experiment. Each test was carried out for 50000 s.

The glass transition temperature (T_g) of each network was characterized by differential scanning calorimetry (DSC) employing a Mettler Toledo DSC822e. Samples were maintained at 50 °C for 20 min, followed by cooling to –20 °C at a rate of –40 °C/min. The T_gs were determined from the second heating ramp at a 10 °C /min rate using the 1/2 ΔC_p method.

Thermogravimetric analysis (TGA) was performed using a Mettler Toledo TGA/DSC3+. Samples were heated under a nitrogen atmosphere from 25 °C to 600 °C at a 20 °C /min heating rate. The change in weight was recorded as a function of temperature.

Scanning electron microscopy (SEM) samples were prepared by fracturing the PHU–POSS composites and coating them with a 15-nm-thick layer of osmium using an OPC osmium coater. The morphologies of the fractured section of the composites were obtained using a Hitachi S-8030 scanning electron microscope.

Wide-angle X-ray scattering (WAXS) measurements were performed using a Rigaku SmartLab X-ray diffractometer in transmission mode. CuK_α radiation was operated at 40 kV and 35 mA. The scattering angle (2θ) covered the range from 3° to 60° with a 0.05° step. The *d*-

spacing can be calculated using Bragg's law, where $\lambda = 2d\sin\theta$; $\lambda = 0.154$ nm for CuK_α radiation.

3. Results and Discussion

3.1. Synthesis of POSS-CC and PHU–POSS network nanocomposites. POSS-CC was synthesized by CO_2 fixation of EP0405 in the presence of a catalytic amount of TBAI at 80 °C. EP0405 is a commercially available glycidyl-ether-terminated POSS consisting of a mixture of POSS with different cage sizes (containing 8–12 silicon atoms per cage and thus 8–12 functional groups). The reaction progress was periodically checked by ^{1}H NMR spectroscopy. Fig. S2 shows the ^{1}H NMR spectrum of POSS-CC. After ~5 days of reaction, the complete disappearance of proton signals at 2.70–3.00 ppm associated with epoxy units and the appearance of signals at 4.50–4.87 ppm associated with the cyclic carbonate moiety indicate complete conversion of epoxy groups into cyclic carbonate groups. POSS-CC was obtained as a light-yellow, high-viscosity liquid. The exact cyclic carbonate content of POSS-CC was determined via ^{1}H NMR spectroscopy with 1,2,4,5-tetrachlorobenzene as an internal reference to be 0.006 mol/g.

The PHU–POSS network composites were synthesized following the synthesis route shown in Fig. S1. The FTIR spectra of the as-synthesized materials are shown in Fig. S4 and Fig. S5. PHUs were successfully synthesized as indicated by the disappearance of the carbonate peak at ∼1780 cm^{-1} and the appearance of the urethane carbonyl stretch at 1700−1730 cm^{-1} and the hydroxyl stretch at 3500−3100 cm^{-1}. In Fig. S5, nearly no signal associated with cyclic carbonates can be observed at ∼1780 cm^{-1} in the as-synthesized PHU-POSS-5, indicating a nearly 100% conversion. In Fig. S4, a small peak exists at ∼1780 cm^{-1} in the as-synthesized PHU-POSS-10, indicating that a small level of unreacted cyclic carbonate remained. This slightly reduced conversion of PHU-POSS-10 relative to PHU-POSS-5 can be explained by the fact that PHU-POSS-10 contains a higher fraction of the multifunctional POSS-CC cross-linker (with 8−12 reactive cyclic carbonate groups). After most of the functional groups undergo cross-

linking, the reduced network mobility will make it more difficult for remaining unreacted cyclic carbonate groups to participate in the reaction.

3.2. Microstructure of PHU–POSS network nanocomposites. It is possible that POSS can aggregate and crystallize. To address the microstructure of the PHU–POSS network composites, WAXS analysis was performed to determine the crystalline degree of the samples. Fig. S6 shows the WAXS patterns of the neat PHU and PHU–POSS network composites. The intensity trace of the neat PHU network shows no peak up to a 2θ value of 60°, indicating the absence of crystalline order. For both PHU-POSS-5 and PHU-POSS-10, the WAXS patterns exhibit a broad peak at ~20° 2θ, which corresponds to a *d*-spacing of ~0.44 nm. Since the average core size of POSS is ~0.50 nm, this broad, amorphous peak is consistent with the presence of POSS nanofillers. Regardless of the POSS loading content, sharp, distinct peaks corresponding to crystalline phases are not present in the WAXS patterns of the PHU–POSS composites, indicating that the nanocomposites are amorphous. The lack of crystalline order associated with high POSS loading content in our samples is consistent with the results reported by Romo-Uribe, in which the POSS-methyl methacrylate nanocomposites remain amorphous with up to 45 wt% POSS content [46].

The morphology of the 1st molded PHU-POSS-10 network which contains 10 wt% POSS-CC was further examined using SEM. The SEM images (see Fig. S7) show no indication of POSS phase separation or aggregation. The POSS-CCs are covalently attached to the PHU matrix and serve as both nanofillers and cross-linkers within the matrix. The fact that each nanofiller can be covalently attached at up to 8–12 reactive sites with the matrix rather than doped into the matrix is conducive to a well-dispersed state. Indeed, Blattmann and Mülhaupt have used the same multifunctional POSS-CC used in this study to synthesize hybrid PHU–POSS thermosets and reported that minor or no phase separation was present with 13.5 wt% POSS-CC; significant phase separation was only observed with 23 wt% POSS-CC [73], far above the 10 wt% POSS loading in our study. Thus, it is reasonable that our systems are not exhibiting POSS nanoaggregates. We note that the number of reactive sites associated with each

nanofiller can also be important in the dispersion state. Liu et al. [75] synthesized PHUs with reactive trifunctional POSS cyclic carbonates; their nanocomposites exhibited 20–40 nm POSS aggregates at 5 wt% POSS content.

3.3. Effect of POSS incorporation on thermal properties of PHU networks. Neat PHU networks and PHU–POSS network composites were synthesized following the reaction route shown in Fig. 1. 10 mol% DMAP with respect to amine functional groups was added into the reaction mixture to facilitate the dynamic chemistries during the reprocessing process. POSS-CC was used as covalently attached nanofillers and was incorporated into neat PHU matrix at 0 wt%, 5 wt% (1.2 wt% of Si−O), and 10 wt% (2.5 wt% of Si−O) loading (weight percentage is with respect to the total weight of network).

The cross-linked nature of the networks was confirmed by equilibrium swelling tests in DCM (Table S1). Fig. 2 shows the glass transition temperatures (T_gs) of as-synthesized networks determined by DSC. According to DSC characterization results, T_g decreases from 21°C for the neat PHU network to 14 °C for PHU-POSS-5 and further to 10 °C for PHU-POSS-10. The

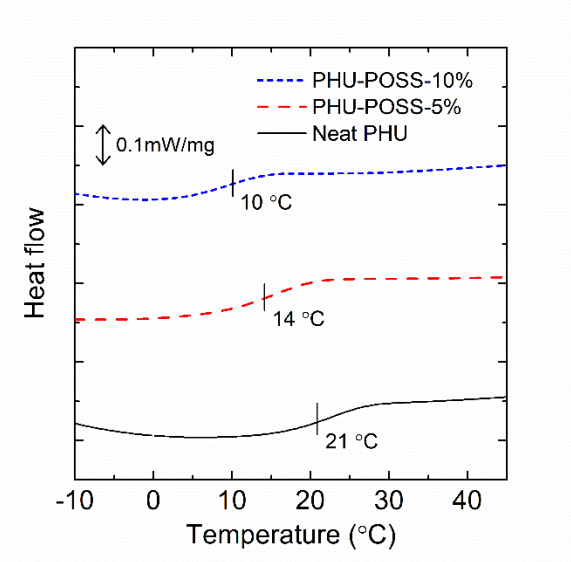

Fig. 2. Glass transition temperatures of as-synthesized neat PHU and PHU–POSS network composites determined by differential scanning calorimetry.

decrease in T_g with increasing POSS loading is related to the long-chain, flexible structure of the side groups connected to the POSS core. Low T_g is a desirable characteristic for thermosets used for elastomer applications. The incorporation of conventional fillers generally leads to increase in T_g, which could negatively impact the performance of elastomers at lower temperatures. In our systems, the employment of POSS-CC offers an advantage of improving the mechanical properties of neat PHU networks while maintaining relatively low T_gs of the materials. In addition, as shown in Table S2, no change in T_g breadth was observed with increasing POSS content, indicating that there is no significant change in overall network homogeneity associated with POSS incorporation.

Thermogravimetric analysis (TGA) was conducted to evaluate the effect of POSS incorporation on thermal decomposition temperatures and thermal stability of dynamic PHU networks (Fig. 3). The decomposition temperatures (T_d) corresponding to a 5 % weight loss for the neat PHU network is 288 ± 3 °C. With the addition of POSS, T_d increases to 296 ± 1 °C for PHU-POSS-5 and further increases to 305 ± 3 °C for PHU-POSS-10. These results suggest that

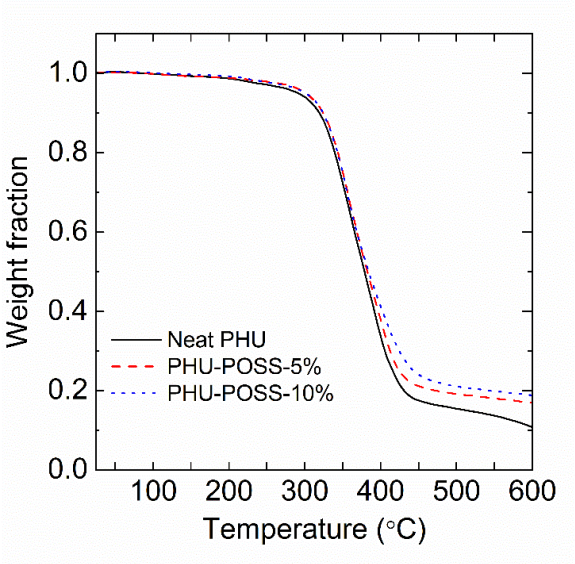

Fig. 3. Thermogravimetric analysis of as-synthesized neat PHU and PHU–POSS network composites.

the thermal stability of PHU networks can be enhanced by incorporating POSS as nanofillers. Upon heating, dynamic PHU networks can undergo two types of dynamic chemistries, which are associative transcarbamoylation exchange reactions and dissociative reversible cyclic carbonate aminolysis reactions (Fig. 4) [27,72]. The reversion of hydroxyurethane linkages to carbonate and amine moieties will decross-link the network structure and accelerate the decomposition process of the materials. By replacing a small part of the trifunctional carbonate cross-linker THPMTC with POSS-CC possessing eight to twelve reactive carbonate functional groups, the materials can withstand the loss of more chains upon heating while maintaining a cross-linked nature.

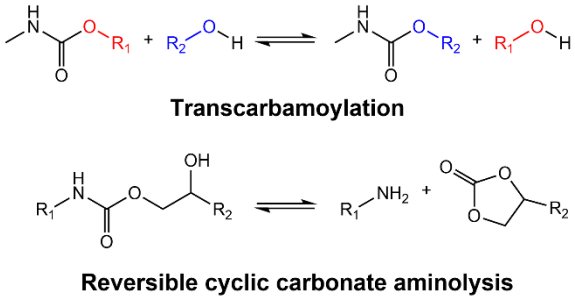

Fig. 4. Transcarbamoylation and reversible cyclic carbonate aminolysis reactions.

3.4. Effect of POSS incorporation on thermomechanical properties and reprocessability of PHU networks. Reprocessing of neat PHU networks and PHU–POSS network composites was performed by cutting the materials into small pieces and compressing them into films using a high-temperature compression mold. DMA characterizations were performed to evaluate the recovery of thermomechanical properties after each reprocessing step. Fig. 5 shows the DMA results of the 1st molded and 2nd molded neat PHU networks. The reprocessing time and temperature for neat PHU networks was 2 h at 140 °C, and the same condition was employed for both the 1st and the 2nd reprocessing cycles. As shown in Fig. 5, the *E*' curves for both samples display a rubbery plateau region a few tens of degrees above T_g, confirming their cross-linked nature. The *E*' rubbery plateau moduli determined at 60 °C, 70 °C, and 80 °C are summarized in Table 1. Within experimental error, the rubbery plateau *E*' values of the 2nd molded sample are

identical to the values of the 1st molded sample at all three temperatures. According to Flory's ideal rubber elasticity, the rubbery plateau modulus is proportional to the cross-link density of a network material [76]. Therefore, these results indicate that neat PHU networks derived from THPMTC and D400 can undergo at least two molding or reprocessing cycles with complete recovery of cross-link density.

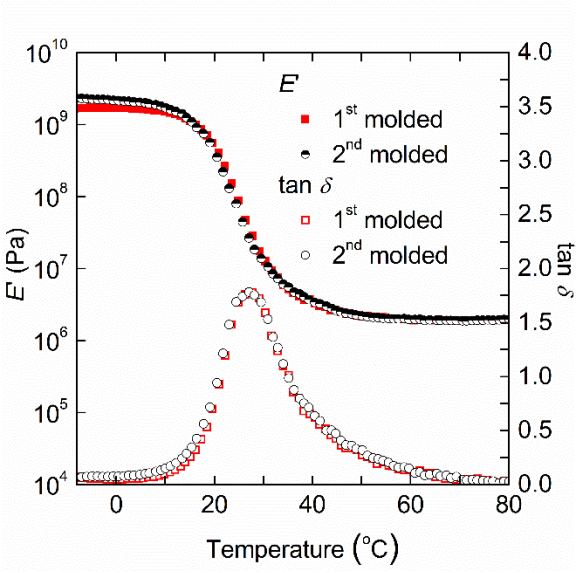

Fig. 5. Dynamic mechanical analysis results of 1st and 2nd molded neat PHU networks.

Table 1. Rubbery plateau moduli (*E*') of the neat PHU network and PHU–POSS network composites at 60 °C, 70 °C, and 80 °C.

sample		*E*' at 60 °C	*E*' at 70 °C	*E*' at 80 °C
Neat PHU	1st molded	1.98 ± 0.02	1.90 ± 0.01	1.93 ± 0.01
	2nd molded	1.96 ± 0.10	1.85 ± 0.11	1.89 ± 0.11
PHU-POSS-5	1st molded	2.04 ± 0.03	2.06 ± 0.02	2.11± 0.01
	2nd molded	2.03 ± 0.16	2.08± 0.15	2.13 ± 0.14
PHU-POSS-10	1st molded	2.43 ± 0.11	2.49 ± 0.02	2.56 ± 0.03
	2nd molded	2.35 ± 0.06	2.42 ± 0.05	2.45 ± 0.06

Fig. 6 shows the DMA curves of the 1st and 2nd molded PHU-POSS-5 samples. The same reprocessing condition of 2 h at 140 °C that was used for neat PHU networks was employed for PHU-POSS-5. As evidenced by the well-overlapped *E*' curves on Fig. 6 and the identical rubbery plateau *E*' values (within error) determined at 60 °C, 70 °C, and 80 °C shown in Table 1, PHU-POSS-5 can also undergo reprocessing without any loss in cross-link density. With 5 wt% POSS incorporated into the materials, PHU-POSS-5 samples exhibit comparable reprocessability to neat PHU networks, indicating that the introduction of a small amount of POSS as nanofillers into a dynamic covalent PHU matrix does not lead to negative impacts.

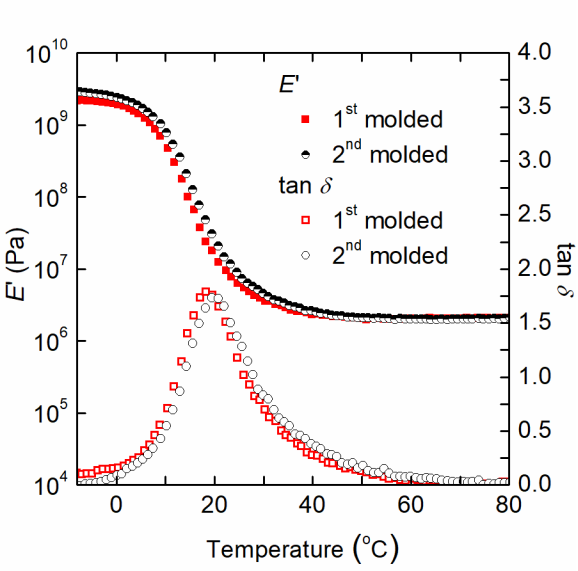

Fig. 6. Dynamic mechanical analysis results of 1st and 2nd molded PHU-POSS-5 samples.

To reprocess the composites PHU-POSS-10 containing 10 wt% POSS, we first used the reprocessing condition of 2.5 h at 140 °C for both the 1st and the 2nd reprocessing cycles, where 2.5 h is the minimum time that is required for the as-synthesized materials to heal into a consolidated film without visible defects (considered as 1st molded samples). The reprocessing time is slightly increased relative to neat PHU networks and PHU-POSS-5, indicating that POSS incorporation introduces additional barriers for chain dynamics at relatively high POSS loading. DMA characterization of the reprocessed samples suggests that there is a small but significant

~10% decrease in rubbery plateau *E*' (Fig. S8) from the 1st molded PHU-POSS-10 samples to the 2nd molded PHU-POSS-10 samples. Without changing the 2.5 h reprocessing time from as-synthesized PHU-POSS-10 to 1st molded PHU-POSS-10, we shortened the reprocessing time from the 1st molded materials to the 2nd molded materials by 1 h. We note that based on our previous experience of reprocessing dynamic PHU networks by compression molding, the minimum time that is required to compress as-synthesized materials into 1st molded materials always appears longer than the minimum time that is required to compress 1st molded materials into 2nd molded materials. This may occur because the as-synthesized materials are in the form of chunks, whereas the 1st molded materials are in the form of thin sheets and hence are easier to be compressed into films again. Therefore, even though 2.5 h is the minimum time that is necessary to obtain well-healed 1st molded PHU-POSS-10 samples, we can still obtain consolidated, well-healed 2nd molded materials by reprocessing the 1st molded samples for only 1.5 h.

After we shortened the reprocessing time of the 2nd cycle, we performed DMA characterization again to determine if there was any improvement in property recovery. As shown in Fig. 7, the *E*' curve of the 2nd molded PHU-POSS-10 samples overlaps reasonably well with the curve of the 1st molded samples, indicating that after shortening the reprocessing time of the 2nd cycle relative to the 1st cycle, PHU-POSS-10 can successfully undergo two reprocessing

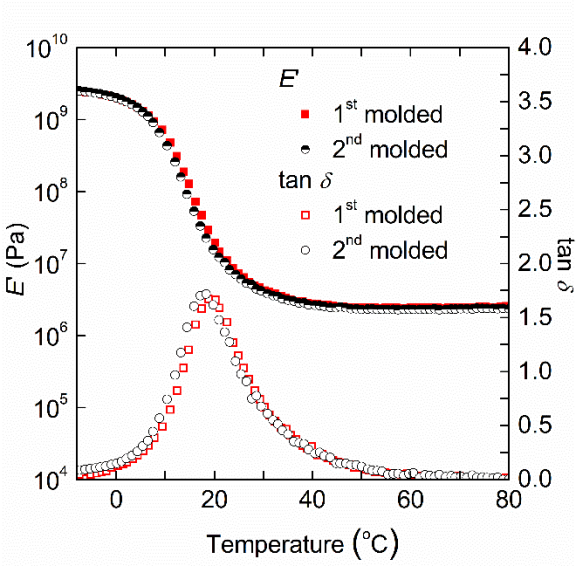

Fig. 7. Dynamic mechanical analysis results of 1st and 2nd molded PHU-POSS-10 samples.

cycles with 100% recovery of cross-link density. To reveal the underlying cause of the loss in cross-link density associated with long reprocessing time, we performed FTIR spectroscopy on as-synthesized PHU-POSS-10, 1st molded PHU-POSS-10 reprocessed by 2.5 h, 2nd molded PHU-POSS-10 reprocessed by 1.5 h, and 2nd molded PHU-POSS-10 reprocessed by 2.5 h. As shown in Fig. S4, on the FTIR spectrum of as-synthesized PHU-POSS-10, no peak exists near ~1660 cm^{-1} (related to C=O stretching vibrations of urea groups). After the materials are reprocessed at 140 °C for 2.5 h to yield 1st molded samples, a shoulder appears at ~1660 cm^{-1} in the spectrum of the 1st molded PHU-POSS-10, indicating the appearance of small amount of urea groups. The urea peak becomes more obvious when the 1st molded materials are further reprocessed for 1.5 h (the red curve in Fig. S4). In the spectrum of the 2nd molded sample obtained with 2.5 h of reprocessing which exhibits significant property loss (the blue curve in Fig. S4), the urea peak is even more prominent.

Boisson et al. has reported the formation of urea in the presence of basic catalysts during PHU synthesis at elevated temperatures [77]. According to the mechanism they proposed, free amine groups liberated from the reverse cyclic carbonate aminolysis reactions can further be deprotonated by a basic catalyst and attack the electrophilic center of another urethane linkage, leading to the formation of urea groups and difunctional alcohols. We hypothesized that in our systems, the property loss in 2nd molded PHU-POSS-10 associated with long reprocessing time is also caused by urea formation at high reprocessing temperature. Fig. S5 shows the FTIR spectra of as-synthesized and reprocessed PHU-POSS-5 samples. As the total reprocessing time increases with more reprocessing cycles, the urea peak progressively grows. However, based on the relatively small size of the urea peak and the 100% property recovery of PHU-POSS-5 determined by DMA characterization, such a low level of side reactions does not significantly affect the reprocessability of the materials. In the case of PHU-POSS-10, when 2.5 h of reprocessing time is used for both reprocessing cycles, the total reprocessing time is 5 h; such extended exposure of the materials at high temperature (140 °C) leads to significant level of urea

formation and consequently leads to decrease in cross-link density after recycling. When the total reprocessing time is shortened to 4 h, even though there is still a small amount of urea formed during reprocessing, such a small level of side reactions does not influence the bulk thermomechanical properties of PHU networks similar to the case of PHU-POSS-5.

Fig. 8 compares the *E*' curves of 1st molded neat PHU, PHU-POSS-5, and PHU-POSS-10. With increasing POSS content, the storage modulus in both the glassy state (i.e., ≤ 0 °C) and the rubbery plateau region (i.e., ≥ 60 °C) increases significantly. As determined from the *E*' values summarized in Table 1, at 80 °C where the materials are well in the rubbery plateau regime, 1st molded PHU-POSS-5 exhibits slightly enhanced *E*' (by ~9%) compared to the neat PHU network, whereas 1st molded PHU-POSS-10 exhibits a significant enhancement of ~30% in *E*'. Equilibrium swelling tests (Table S1) also show that the networks swell less with increasing POSS loading, consistent with a higher degree of cross-linking after POSS incorporation. These

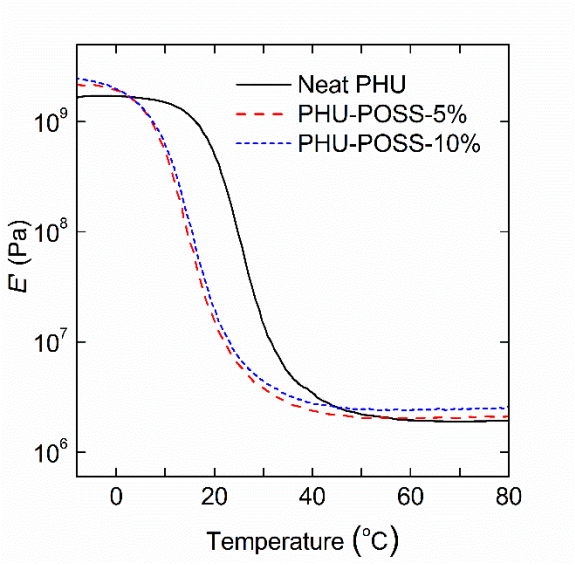

Fig. 8. Temperature dependence of the storage moduli of 1st molded neat PHU, PHU-POSS-5%, and PHU-POSS-10%.

results indicate that the incorporation of POSS as nanofillers is an effective way to improve the modulus of dynamic PHU networks well into the glassy state or the rubbery plateau regime while maintaining good reprocessability. (The fact that *E*' is significantly higher for neat PHU

than for the nanocomposites in the temperature range of 5–45 °C simply reflects the higher T_g of neat PHU, which is caused by the long-chain, flexible structure of the side groups connected to the POSS core resulting in plasticization of the nanocomposites.) To understand how these materials respond to large tensile stresses, future studies are warranted to characterize the tensile properties of PHU−POSS composites including tensile strength and strain-at-break.

3.5. Effect of POSS incorporation on stress relaxation behavior of PHU networks. The ability to relax external stress under appropriate conditions is a defining characteristic of dynamic polymer networks. For PHU networks, stress relaxation at elevated temperatures is enabled by simultaneous associative transcarbamoylation exchange reactions and dissociative reversible cyclic carbonate aminolysis reactions. We have characterized the effect of POSS incorporation on stress relaxation of dynamic PHU networks by DMA. Stress relaxation tests at 140−170 °C were conducted under a strain of 5%. Fig. 9 shows the decay of stress relaxation modulus as a function of relaxation time at different temperatures. Regardless of the loading of POSS, at all tested temperatures, the PHU–POSS composites relax much more slowly than the neat PHU network. It is generally recognized that when non-reactive nanofillers are incorporated into a network matrix, the mobility of the network is typically reduced because of the adsorption of polymer chains onto filler surface at the polymer−filler interfaces. For our PHU–POSS nanocomposites, the impact on network mobility from chain adhesion is minimized by using POSS that have extremely small surface-to-volume ratio as reinforcing agents. However, when part of the trifunctional carbonates THPMTC was replaced with POSS molecules possessing 8 to 12 reactive carbonate groups, the resulting networks are much denser and more inflexible compared with the neat PHUs, and therefore the stress relaxation rate is still retarded. Nevertheless, with increasing temperature, the difference in stress relaxation rate between neat PHU networks and PHU–POSS composites is diminished, possibly because at high temperatures, the stress relaxation process of PHU networks is achieved predominantly by dissociative reverse cyclic carbonate aminolysis reaction, so all systems are equally liquid-like and highly flexible.

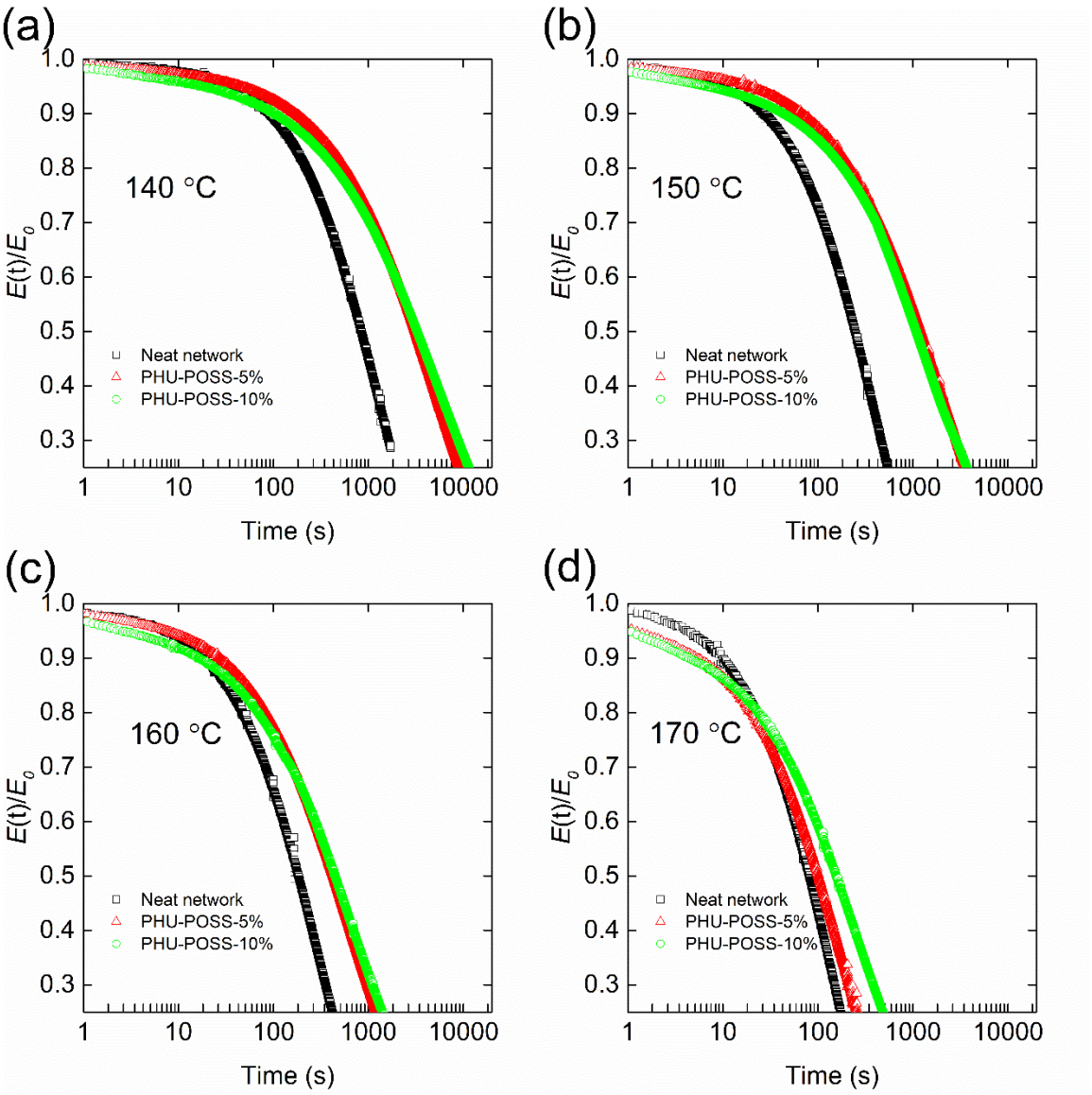

Fig. 9. Stress relaxation curves of neat PHU networks and PHU–POSS network composites at (a) 140 °C, (b) 150 °C, (c) 160 °C, and (d) 170 °C.

We note that with increasing POSS loading, although the average stress relaxation time is increased significantly, the systems containing more POSS exhibit relatively faster relaxations at the initial stage of the stress relaxation experiments. This observation suggests that the relaxation of PHU–POSS composites comprises a multitude of relaxation modes, and a single Maxwell element is insufficient to model the process. To model the effect of POSS incorporation on the stress relaxation of PHU networks, we used the Kohlrausch–Williams–Watts (KWW) stretched

exponential decay function to fit the stress relaxation data. The KWW stretched exponential decay function is expressed as follows [72,78,79]:

$$\frac{\sigma(t)}{\sigma_0} = \exp\{-\left(\frac{t}{\tau^*}\right)^{\beta}\} \quad (2)$$

where $\sigma(t)/\sigma_0$ is the normalized stress at time t, τ^* is the characteristic relaxation time, and β is the exponent that controls the shape of the stretched exponential decay and reflects the breadth of the relaxation distribution. β takes values in the range $0 < \beta \leq 1$, with $\beta = 1$ corresponding to a single-exponential decay response and $\beta \ll 1$ indicating an extremely broad distribution of relaxation times. For a KWW decay, the average relaxation time, $\langle\tau\rangle$, is given by [72,79]

$$\langle\tau\rangle = \frac{\tau^* \Gamma(\frac{1}{\beta})}{\beta} \quad (3)$$

where Γ is the Gamma function. Table S4 shows the detailed fitting results obtained from both KWW stretched exponential decay and single-exponential decay analyses for neat PHU networks and PHU–POSS composites. For neat PHU networks, β increases slightly with increasing temperature, and the value becomes very close to 1 at 170 °C, indicating a nearly single-exponential decay response. With increasing POSS content of the materials, β decreases at all tested temperatures, suggesting a broadened distribution of relaxation times and a more complex relaxation mode with higher POSS loading.

Fig. 10 shows the Arrhenius plot of $\langle\tau\rangle$ over the temperature range of 140 °C ≤ T ≤ 170 °C for determining the apparent activation energy ($E_{a,\tau}$) of stress relaxation; the detailed results are summarized in Table 2. The $E_{a,\tau}$ of neat PHU networks was calculated to be 121 kJ/mol, which is in reasonable agreement with values reported by other studies on dynamic PHU networks [72,80]. When POSS molecules are added to the neat PHU matrix, $E_{a,\tau}$ increases dramatically, indicating a stronger temperature dependence of the relaxation process. As shown in Fig. 10, at low temperatures, PHU–POSS composites exhibit significantly longer average relaxation times than the neat PHU network. This occurs because when part of the original trifunctional cross-linker THPMTC is replaced with the multifunctional POSS-CC cross-linker with 8–12 functional groups, the composites have a much more restricted network structure and

hence substantially reduced flexibility at low temperatures than the neat PHU network. With increasing temperature, the average relaxation times of the three systems become similar. At sufficiently high temperatures, all networks are far above their T_gs, and the reverse cyclic carbonate aminolysis reaction leads to a less cross-linked state. Therefore, the dynamics of the three systems become more alike. These above-mentioned effects result in a stronger temperature dependence of the relaxation process and thus an increase in $E_{a,\tau}$ after POSS incorporation. The secondary effect of POSS incorporation on $E_{a,\tau}$ values is that PHU-POSS-5 exhibits a greater $E_{a,\tau}$ value than PHU-POSS-10. This is because the stress relaxation process of dynamic polymer network depends on both the activation energies of the dynamic chemistries and the viscoelastic behavior of the materials. The POSS-CC cross-linker has flexible side chains which result in a decrease in overall T_g of the materials with increasing POSS-CC content. Therefore, at the same temperature, PHU-POSS-10 networks are more liquid-like compared to PHU-POSS-5. This subsequently leads to a smaller temperature dependence or a smaller $E_{a,\tau}$ of the stress relaxation process for the PHU-POSS-10 than PHU-POSS-5.

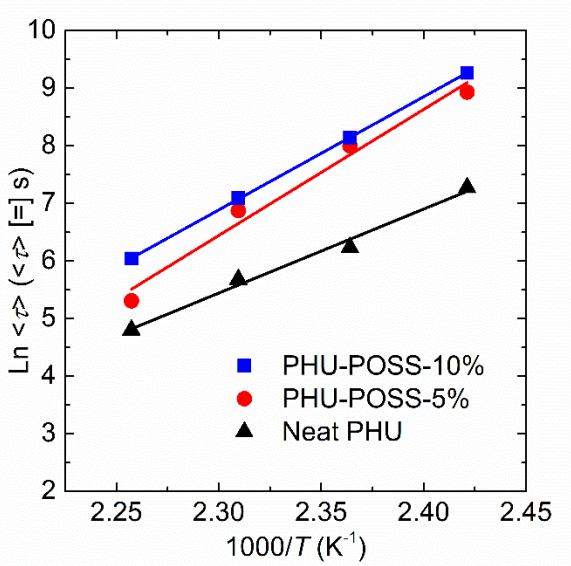

Fig. 10. Arrhenius apparent activation energy of stress relaxation for the neat PHU networks and PHU-POSS network composites.

Table 2. $<\tau>$ at 140 °C and apparent activation energy of stress relaxation of the 1st molded neat PHU network and PHU–POSS network composites.

sample	$<\tau>$ at 140 °C (s)	apparent activation energy (kJ/mol)
Neat PHU	1440	121
PHU-POSS-5%	7530	182
PHU-POSS-10%	10540	163

3.6. Creep performance of neat PHU network and PHU–POSS network composites.

Because of their dynamic nature, there is a potential shortcoming of CANs related to creep during use at elevated temperature, which is undesirable for many applications [33]. Creep refers to the continuous, time-dependent deformation of materials under constant stress [81]. Conventional thermosets composed of fixed covalent bonds are intrinsically creep-resistant [82–84] whereas CANs are susceptible to creep especially at elevated temperature but still well below the reprocessing temperature, as demonstrated in numerous studies [21,85–88]. To arrest elevated temperature creep of CANs, an effective approach is to employ a dynamic chemistry with high activation energy and strong temperature dependence such that the dynamic mechanism remains relatively inactive and allows for creep resistance at temperatures not too far below the reprocessing temperature [11,13,89].

A previous study involving alkoxyamine dynamic chemistry has indicated that the elevated-temperature creep resistance of CANs should not be affected significantly by network details or by the presence or absence of fillers [11]. To determine the creep response of our dynamic PHU network and the potential impact of POSS incorporation on the response, linear viscoelastic creep tests were performed at 80 °C and 90 °C, some 50−60 °C below the reprocessing temperature, under a constant 3.0 kPa shear stress. At both temperatures, the materials are well above their T_gs and in the rubbery plateau regime. Fig. 11 shows the creep

responses for the neat PHU network and PHU–POSS network composites. For all systems, the time-dependent creep is extremely small after 50000 s (~14 h). Creep strain values ($\Delta\varepsilon$) summarized in Table 3 were determined as the difference in strain at t = 50000 s and t = 1800 s (i.e., $\Delta\varepsilon = \varepsilon_{50000} - \varepsilon_{1800}$) such that the values only reflect pure creep, instead of delayed elastic deformation [83]. The creep strain values of neat PHU and PHU–POSS composites are only 0.003 (i.e., 0.3%) at 80 °C and 0.005 (i.e., 0.5%) at 90 °C, which are extremely small and comparable to the response associated with permanently cross-linked static networks [82–84]. These results indicate that the hydroxyurethane dynamic chemistry is very effective in suppressing long-term elevated-temperature creep at 80–90 °C, and this excellent creep-resistant feature is not affected significantly by POSS incorporation in which POSS serves as a fraction of the dynamic covalent crosslinks in the network.

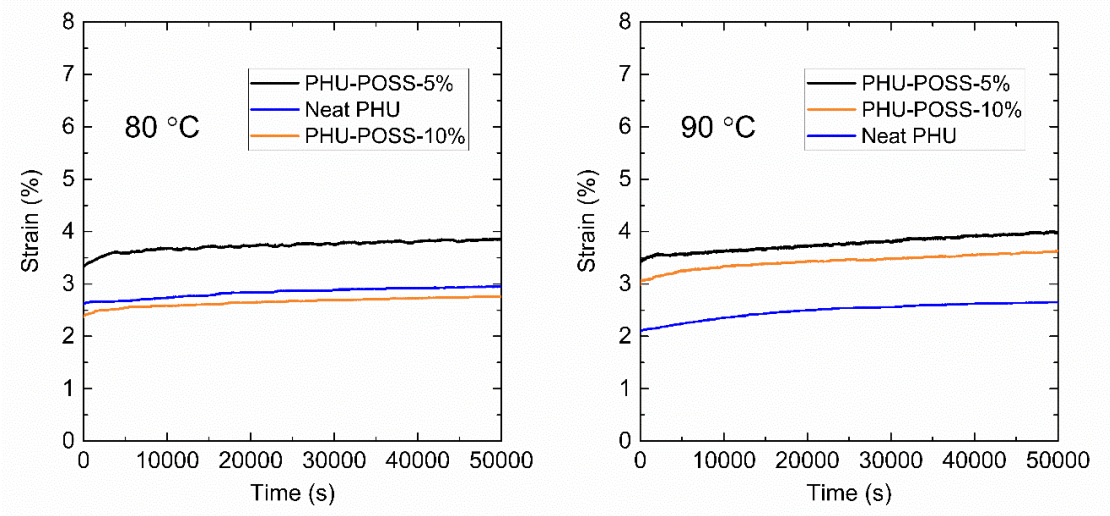

Fig. 11. Creep responses for the neat PHU network and PHU–POSS network composites at (a) 80 °C and (b) 90 °C.

Finally, we note that in Fig. 11 the instantaneous strains do not strictly follow a decreasing trend with increasing POSS content. Based on our previous experience with shear creep measurements on solid-state samples using a parallel-plate fixture, the instantaneous strain values are strongly impacted by the surface roughness of the samples. The samples need to be

cured into a disk shape using a high-temperature compression molding device before the creep measurements. If the disks have very smooth surfaces after curing, the instantaneous strain usually reflects the trend in modulus very well. However, if the samples have relatively rough surfaces, the normal force acting on the samples needs to be adjusted until a good contact with the parallel plate is achieved, and this kind of adjustment usually results in impacts on the instantaneous strain values. Nevertheless, creep is a time-dependent response, and the creep strain is determined from the absolute change in strain values over time, so the instantaneous strain value should not have impacts on the time-dependent strain that is associated with creep.

Table 3. Creep strain, $\Delta\varepsilon$, of neat PHU network and PHU–POSS network composites at different temperatures under a constant creep stress of 3.0 kPa.

sample	$\Delta\varepsilon$ at 80 °C	$\Delta\varepsilon$ at 90 °C
Neat PHU	0.003	0.004
PHU-POSS-5%	0.003	0.004
PHU-POSS-10%	0.003	0.005

Note: Creep strain is taken as $\Delta\varepsilon = \varepsilon_{50000\ s} - \varepsilon_{1800\ s}$.

4. Conclusion

We have used POSS with cyclic carbonate end groups as covalently attached nanofillers to develop reprocessable PHU–POSS network composites. The incorporation of POSS leads to enhanced thermal stability and significantly enhanced rubbery plateau modulus of the networks relative to the PHU without nanofiller. Because of the inherent dynamic nature of hydroxyurethane linkage, the PHU–POSS network composites can be melt-reprocessed at elevated temperatures. With up to 10 wt% POSS loading, PHU–POSS network composites exhibit excellent reprocessability and can undergo multiple reprocessing cycles with 100% recovery of cross-link density; such excellent property recovery has not been achieved before with dynamic PHU network composites derived from conventional silica nanoparticles. The

stress relaxation activation energy $E_{a,\tau}$ associated with the average relaxation time of the networks was determined using the data from the high-temperature stress relaxation tests. It was found that $E_{a,\tau}$ increases when POSS molecules are incorporated into the neat PHU matrix, suggesting an increase in relaxation barrier. Lastly, the linear viscoelastic creep response of the neat PHU network and PHU–POSS network composites was characterized via creep tests under a constant 3.0 kPa shear stress. We found that dynamic PHU networks exhibit nearly no creep over 50000 s at temperatures of 80−90 °C, indicating the hydroxyurethane dynamic chemistry is effective in arresting elevated-temperature creep, regardless of the presence of nanofillers. This study highlights the advantages and effectiveness of POSS molecules for fabricating high-performance reprocessable network composites.

CRediT authorship contribution statement

Sumeng Hu: Conceptualization, Methodology, Investigation, Formal analysis, Data Curation, Writing - Original Draft. **Xi Chen:** Conceptualization, Writing - Review & Editing. **Mohammed A. Bin Rusayyis:** Methodology, Writing - Review & Editing. **Nathan S. Purwanto:** Investigation. **John M. Torkelson:** Supervision, Project administration, Funding acquisition, Writing - Review & Editing.

Declaration of competing interests

The authors declare that they have no known competing financial interests or personal relationships that could have appeared to influence the work reported in this paper.

Acknowledgments

This work was financially supported by discretionary funds from a Walter P. Murphy Professorship and by the U.S. Department of Energy's Office of Energy Efficiency and Renewable Energy (EERE) under the Bioenergy Technologies Office Award Number DE-EE0008928.

References

[1] C.J. Kloxin, T.F. Scott, B.J. Adzima, C.N. Bowman, Covalent adaptable networks (CANS): a unique paradigm in cross-linked polymers, Macromolecules 43 (2010) 2643–2653. https://doi.org/10.1021/ma902596s

[2] C.J. Kloxin, C.N. Bowman, Covalent adaptable networks: smart, reconfigurable and responsive network systems, Chem. Soc. Rev. 42 (2013) 7161–7173. https://doi.org/10.1039/C3CS60046G

[3] W. Zou, J. Dong, Y. Luo, Q. Zhao, T. Xie, Dynamic covalent polymer networks: from old chemistry to modern day innovations, Adv. Mater. 29 (2017) 1606100. https://doi.org/10.1002/adma.201606100

[4] X. Chen, M.A. Dam, K. Ono, A. Mal, H. Shen, S.R. Nutt, K. Sheran, F. Wudl, A thermally re-mendable cross-linked polymeric material, Science 295 (2002) 1698–1702. https://doi.org/10.1126/science.1065879

[5] Q. Zhang, S. Wang, B. Rao, X. Chen, L. Ma, C. Cui, Q. Zhong, Z. Li, Y. Cheng, Y. Zhang, Hindered urea bonds for dynamic polymers: An overview, React. Funct. Polym. 159 (2021) 104807. https://doi.org/10.1016/j.reactfunctpolym.2020.104807

[6] H. Ying, Y. Zhang, J. Cheng, Dynamic urea bond for the design of reversible and self-healing polymers, Nat. Commun. 5 (2014) 3218. https://doi.org/10.1038/ncomms4218

[7] Y. Zhang, H. Ying, K.R. Hart, Y. Wu, A.J. Hsu, A.M. Coppola, T.A. Kim, K. Yang, N.R. Sottos, S.R. White, J. Cheng, Malleable and recyclable poly(urea-urethane) thermosets bearing

hindered urea bonds, Adv. Mater. 28 (2016) 7646–7651.
https://doi.org/10.1002/adma.201601242
[8] M.A. Bin Rusayyis, J.M. Torkelson, Reprocessable and recyclable chain-growth polymer networks based on dynamic hindered urea bonds, ACS Macro Lett. 11 (2022) 568–574.
https://doi.org./10.1021/acsmacrolett.2c00045
[9] H. Otsuka, Reorganization of polymer structures based on dynamic covalent chemistry: polymer reactions by dynamic covalent exchanges of alkoxyamine units, Polym. J. 45 (2013) 879–891. https://doi.org/10.1038/pj.2013.17
[10] K. Jin, L. Li, J.M. Torkelson, Recyclable crosslinked polymer networks via one-step controlled radical polymerization, Adv. Mater. 28 (2016) 6746–6750.
https://doi.org/10.1002/adma.201600871
[11] L. Li, X. Chen, K. Jin, M.A. Bin Rusayyis, J.M. Torkelson, Arresting elevated-temperature creep and achieving full cross-link density recovery in reprocessable polymer networks and network composites via nitroxide-mediated dynamic chemistry, Macromolecules 54 (2021) 1452–1464. https://doi.org/10.1021/acs.macromol.0c01691
[12] M.A. Bin Rusayyis, J.M. Torkelson, Recyclable polymethacrylate networks containing dynamic dialkylamino disulfide linkages and exhibiting full property recovery, Macromolecules 53 (2020) 8367–8373. https://doi.org/10.1021/acs.macromol.0c01539
[13] M.A. Bin Rusayyis, J.M. Torkelson, Reprocessable covalent adaptable networks with excellent elevated-temperature creep resistance: facilitation by dynamic, dissociative bis(hindered amino) disulfide bonds, Polym. Chem. 12 (2021) 2760–2771.
https://doi.org/10.1039/D1PY00187F
[14] D. Montarnal, M. Capelot, F. Tournilhac, L. Leibler, Silica-like malleable materials from permanent organic networks, Science 334 (2011) 965–968.
https://doi.org/10.1126/science.1212648
[15] R.L. Snyder, D.J. Fortman, G.X. De Hoe, M.A. Hillmyer, W.R. Dichtel, Reprocessable acid-degradable polycarbonate vitrimers, Macromolecules 51 (2018) 389–397.

https://doi.org/10.1021/acs.macromol.7b02299
[16] L. Li, X. Chen, K. Jin, J.M. Torkelson, Vitrimers designed both to strongly suppress creep and to recover original cross-link density after reprocessing: quantitative theory and experiments, Macromolecules 51 (2018) 5537–5546. https://doi.org/10.1021/acs.macromol.8b00922
[17] B. Zhang, K. Kowsari, A. Serjouei, M.L. Dunn, Q. Ge, Reprocessable thermosets for sustainable three-dimensional printing, Nat. Commun. 9 (2018) 1831. https://doi.org/10.1038/s41467-018-04292-8
[18] Y. Chen, Z. Tang, X. Zhang, Y. Liu, S. Wu, B. Guo, Covalently cross-linked elastomers with self-healing and malleable abilities enabled by boronic ester bonds, ACS Appl. Mater. Interfaces. 10 (2018) 24224–24231. https://doi.org/10.1021/acsami.8b09863
[19] B. Soman, C.M. Evans, Effect of precise linker length, bond density, and broad temperature window on the rheological properties of ethylene vitrimers, Soft Matter 17 (2021) 3569–3577. https://doi.org/10.1039/D0SM01544J
[20] S. Tajbakhsh, F. Hajiali, M. Marić, Recyclable polymers with boronic ester dynamic bonds prepared by miniemulsion polymerization, ACS Appl. Polym. Mater. 3 (2021) 3402–3415. https://doi.org/10.1021/acsapm.1c00368
[21] W. Denissen, G. Rivero, R. Nicolaÿ, L. Leibler, J.M. Winne, F.E. Du Prez, Vinylogous urethane vitrimers, Adv. Funct. Mater. 25 (2015) 2451–2457. https://doi.org/10.1002/adfm.201404553
[22] W. Denissen, M. Droesbeke, R. Nicolaÿ, L. Leibler, J.M. Winne, F.E. Du Prez, Chemical control of the viscoelastic properties of vinylogous urethane vitrimers, Nat. Commun. 8 (2017) 14857. https://doi.org/10.1038/ncomms14857
[23] J.S.A. Ishibashi, J.A. Kalow, Vitrimeric silicone elastomers enabled by dynamic Meldrum's acid-derived cross-links, ACS Macro Lett. 7 (2018) 482–486. https://doi.org/10.1021/acsmacrolett.8b00166
[24] O. Anaya, A. Jourdain, I. Antoniuk, H. Ben Romdhane, D. Montarnal, E. Drockenmuller, Tuning the viscosity profiles of high-Tg poly(1,2,3-triazolium) covalent adaptable networks by

the chemical structure of the N-substituents, Macromolecules 54 (2021) 3281–3292. https://doi.org/10.1021/acs.macromol.0c02221

[25] Y. Hu, G. Tang, Y. Luo, S. Chi, X. Li, Glycidyl azide polymer-based polyurethane vitrimers with disulfide chain extenders, Polym. Chem. 12 (2021) 4072–4082. https://doi.org/10.1039/D1PY00441G

[26] L. Li, X. Chen, J.M. Torkelson, Covalent adaptive networks for enhanced adhesion: exploiting disulfide dynamic chemistry and annealing during application, ACS Appl. Polym. Mater. 2 (2020) 4658–4665. https://doi.org/10.1021/acsapm.0c00720

[27] X. Chen, L. Li, K. Jin, J.M. Torkelson, Reprocessable polyhydroxyurethane networks exhibiting full property recovery and concurrent associative and dissociative dynamic chemistry via transcarbamoylation and reversible cyclic carbonate aminolysis, Polym. Chem. 8 (2017) 6349–6355. https://doi.org/10.1039/C7PY01160A

[28] Z. Wen, X. Han, B.D. Fairbanks, K. Yang, C.N. Bowman, Development of thiourethanes as robust, reprocessable networks, Polymer 202 (2020) 122715. https://doi.org/10.1016/j.polymer.2020.122715

[29] L. Li, X. Chen, J.M. Torkelson, Reprocessable polymer networks via thiourethane dynamic chemistry: recovery of cross-link density after recycling and proof-of-principle solvolysis leading to monomer recovery, Macromolecules 52 (2019) 8207–8216. https://doi.org/10.1021/acs.macromol.9b01359

[30] X. Chen, S. Hu, L. Li, J.M. Torkelson, Dynamic covalent polyurethane networks with excellent property and cross-link density recovery after recycling and potential for monomer recovery, ACS Appl. Polym. Mater. 2 (2020) 2093–2101. https://doi.org/10.1021/acsapm.0c00378

[31] G.M. Scheutz, J.J. Lessard, M.B. Sims, B.S. Sumerlin, Adaptable crosslinks in polymeric materials: resolving the intersection of thermoplastics and thermosets, J. Am. Chem. Soc. 141 (2019) 16181–16196. https://doi.org/10.1021/jacs.9b07922

[32] M.K. McBride, B.T. Worrell, T. Brown, L.M. Cox, N. Sowan, C. Wang, M. Podgorski,

A.M. Martinez, C.N. Bowman, Enabling applications of covalent adaptable networks, Annu. Rev. Chem. Biomol. Eng. 10 (2019) 175–198. https://doi.org/10.1146/annurev-chembioeng-060718-030217

[33] W. Denissen, J. M. Winne, F.E. Du Prez, Vitrimers: permanent organic networks with glass-like fluidity, Chem. Sci. 7 (2016) 30–38. https://doi.org/10.1039/C5SC02223A

[34] D.J. Fortman, J.P. Brutman, G.X. De Hoe, R.L. Snyder, W.R. Dichtel, M.A. Hillmyer, Approaches to sustainable and continually recyclable cross-linked polymers, ACS Sustainable Chem. Eng. 6 (2018) 11145–11159. https://doi.org/10.1021/acssuschemeng.8b02355

[35] N. Zheng, Y. Xu, Q. Zhao, T. Xie, Dynamic covalent polymer networks: a molecular platform for designing functions beyond chemical recycling and self-healing, Chem. Rev. (2021). https://doi.org/10.1021/acs.chemrev.0c00938

[36] M. Hayashi, Versatile functionalization of polymeric soft materials by implanting various types of dynamic cross-links, Polym J. 53 (2021) 779–788. https://doi.org/10.1038/s41428-021-00474-2

[37] N.D.A. Watuthanthrige, P. Chakma, D. Konkolewicz, Designing dynamic materials from dynamic bonds to macromolecular architecture, Trends Chem. 3 (2021) 231–247. https://doi.org/10.1016/j.trechm.2020.12.005

[38] A.M. Wemyss, C. Ellingford, Y. Morishita, C. Bowen, C. Wan, Dynamic polymer networks: a new avenue towards sustainable and advanced soft machines, Angew. Chem. 133 (2021) 13841–13852. https://doi.org/10.1002/ange.202013254

[39] S. Samanta, S. Kim, T. Saito, A.P. Sokolov, Polymers with dynamic bonds: adaptive functional materials for a sustainable future, J. Phys. Chem. B. 125 (2021) 9389–9401. https://doi.org/10.1021/acs.jpcb.1c03511

[40] T. Wei, K. Jin, J.M. Torkelson, Isolating the effect of polymer-grafted nanoparticle interactions with matrix polymer from dispersion on composite property enhancement: The example of polypropylene/halloysite nanocomposites, Polymer 176 (2019) 38–50. https://doi.org/10.1016/j.polymer.2019.05.038

[41] J.L. Valentín, I. Mora-Barrantes, J. Carretero-González, M.A. López-Manchado, P. Sotta, D.R. Long, K. Saalwächter, Novel experimental approach to evaluate filler−elastomer interactions, Macromolecules 43 (2010) 334–346. https://doi.org/10.1021/ma901999j
[42] K.A. Iyer, G.T. Schueneman, J.M. Torkelson, Cellulose nanocrystal/polyolefin biocomposites prepared by solid-state shear pulverization: superior dispersion leading to synergistic property enhancements, Polymer 56 (2015) 464–475. https://doi.org/10.1016/j.polymer.2014.11.017
[43] M. Qiu, S. Wu, Z. Tang, B. Guo, Exchangeable interfacial crosslinks towards mechanically robust elastomer/carbon nanotubes vitrimers, Compos. Sci. Technol. 165 (2018) 24–30. https://doi.org/10.1016/j.compscitech.2018.06.004
[44] Y. Yang, B. Pöessel, R. Mülhaupt, Graphenated ceramic particles as functional fillers for nonisocyanate polyhydroxyurethane composites, Macromol. Mater. Eng. 305 (2020) 2000203. https://doi.org/10.1002/mame.202000203
[45] D.R. Paul, L.M. Robeson, Polymer nanotechnology: nanocomposites, Polymer 49 (2008) 3187–3204. https://doi.org/10.1016/j.polymer.2008.04.017
[46] A. Romo-Uribe, Viscoelasticity and microstructure of POSS-methyl methacrylate nanocomposites. Dynamics and entanglement dilution, Polymer 148 (2018) 27–38. https://doi.org/10.1016/j.polymer.2018.06.018
[47] Z. Tang, L. Zhang, W. Feng, B. Guo, F. Liu, D. Jia, Rational design of graphene surface chemistry for high-performance rubber/graphene composites, Macromolecules 47 (2014) 8663–8673. https://doi.org/10.1021/ma502201e
[48] A. Legrand, C. Soulié-Ziakovic, Silica–epoxy vitrimer nanocomposites, Macromolecules 49 (2016) 5893–5902. https://doi.org/10.1021/acs.macromol.6b00826
[49] K.A. Iyer, J.M. Torkelson, Importance of superior dispersion versus filler surface modification in producing robust polymer nanocomposites: the example of polypropylene/nanosilica hybrids, Polymer 68 (2015) 147–157. https://doi.org/10.1016/j-polymer.2015.05.015

[50] A. Romo-Uribe and J. D. Lichtenhan, Melt extrusion and blow molding parts-per-million POSS interspersed the macromolecular network and simultaneously enhanced thermo-mechanical and barrier properties of polyolefin films. Polym. Eng. Sci. 61 (2021) 245–257. https://doi.org/10.1002/pen.25572

[51] Y. Liu, Z. Tang, Y. Chen, C. Zhang, B. Guo, Engineering of β-hydroxyl esters into elastomer–nanoparticle interface toward malleable, robust, and reprocessable vitrimer composites, ACS Appl. Mater. Interfaces. 10 (2018) 2992–3001. https://doi.org/10.1021/acsami.7b17465

[52] Z. Huang, Y. Wang, J. Zhu, J. Yu, Z. Hu, Surface engineering of nanosilica for vitrimer composites, Compos. Sci. Technol. 154 (2018) 18–27. https://doi.org/10.1016/j.compscitech.2017.11.006

[53] D.B. Cordes, P.D. Lickiss, F. Rataboul, Recent developments in the chemistry of cubic polyhedral oligosilsesquioxanes, Chem. Rev. 110 (2010) 2081–2173. https://doi.org/10.1021/cr900201r

[54] J. Wang, W. Du, Z. Zhang, W. Gao, Z. Li, Biomass/polyhedral oligomeric silsesquioxane nanocomposites: advances in preparation strategies and performances, J. Appl. Polym. Sci. 138 (2021) 49641. https://doi.org/10.1002/app.49641

[55] Z. Xu, Y. Zhao, X. Wang, T. Lin, A thermally healable polyhedral oligomeric silsesquioxane (POSS) nanocomposite based on Diels–Alder chemistry, Chem. Comm. 49 (2013) 6755–6757. https://doi.org/10.1039/C3CC43432J

[56] D. Zhou, Y. Wang, J. Zhu, J. Yu, Z. Hu, Mechanically strong and highly efficient healable organic/inorganic hybrid dynamic network, Polymer 167 (2019) 202–208. https://doi.org/10.1016/j.polymer.2019.02.018

[57] H. Yang, C. He, T.P. Russell, D. Wang, Epoxy-polyhedral oligomeric silsesquioxanes (POSS) nanocomposite vitrimers with high strength, toughness, and efficient relaxation, Giant. 4 (2020) 100035. https://doi.org/10.1016/j.giant.2020.100035

[58] F. Hajiali, S. Tajbakhsh, M. Marić, Thermally reprocessable bio-based polymethacrylate

vitrimers and nanocomposites, Polymer 212 (2021) 123126. https://doi.org/10.1016/j.polymer.2020.123126
[59] W. Shen, B. Du, H. Zhuo, S. Chen, Recyclable and reprocessable epoxy-polyhedral oligomeric silsesquioxane (POSS)/mesogenic azobenzene/poly (ethylene-co-vinyl acetate) composites with thermal- and light-responsive programmable shape-memory performance, Chem. Eng. J. 428 (2022) 132609. https://doi.org/10.1016/j.cej.2021.132609
[60] J. Guan, Y. Song, Y. Lin, X. Yin, M. Zuo, Y. Zhao, X. Tao, Q. Zheng, Progress in study of non-isocyanate polyurethane, Ind. Eng. Chem. Res. 50 (2011) 6517–6527. https://doi.org/10.1021/ie101995j
[61] H. Blattmann, M. Fleischer, M. Bähr, R. Mülhaupt, Isocyanate- and phosgene-free routes to polyfunctional cyclic carbonates and green polyurethanes by fixation of carbon dioxide, Macromol. Rapid Commun. 35 (2014) 1238–1254. https://doi.org/10.1002/marc.201400209
[62] L. Maisonneuve, O. Lamarzelle, E. Rix, E. Grau, H. Cramail, Isocyanate-free routes to polyurethanes and poly(hydroxy urethane)s, Chem. Rev. 115 (2015) 12407–12439. https://doi.org/10.1021/acs.chemrev.5b00355
[63] M. Kathalewar, A. Sabnis, D. D'Mello, Isocyanate free polyurethanes from new CNSL based bis-cyclic carbonate and its application in coatings, Eur. Polym. J. 57 (2014) 99–108. https://doi.org/10.1016/j.eurpolymj.2014.05.008
[64] A. Cornille, R. Auvergne, O. Figovsky, B. Boutevin, S. Caillol, A perspective approach to sustainable routes for non-isocyanate polyurethanes, Eur. Polym. J. 87 (2017) 535–552. https://doi.org/10.1016/j.eurpolymj.2016.11.027
[64] E.K. Leitsch, G. Beniah, K. Liu, T. Lan, W.H. Heath, K.A. Scheidt, J.M. Torkelson, Nonisocyanate thermoplastic polyhydroxyurethane elastomers via cyclic carbonate aminolysis: critical role of hydroxyl groups in controlling nanophase separation, ACS Macro Lett. 5 (2016) 424–429. https://doi.org/10.1021/acsmacrolett.6b00102
[66] G. Beniah, K. Liu, W.H. Heath, M.D. Miller, K.A. Scheidt, J.M. Torkelson, Novel thermoplastic polyhydroxyurethane elastomers as effective damping materials over broad

temperature ranges, Eur. Polym. J. 84 (2016) 770–783.
https://doi.org/10.1016/j.eurpolymj.2016.05.031
[67] R.H. Lambeth, T.J. Henderson, Organocatalytic synthesis of (poly)hydroxyurethanes from cyclic carbonates and amines, Polymer 54 (2013) 5568–5573.
https://doi.org/10.1016/j.polymer.2013.08.053
[68] A. Gomez-Lopez, F. Elizalde, I. Calvo, H. Sardon, Trends in non-isocyanate polyurethane (NIPU) development, Chem. Comm. 57 (2021) 12254–12265.
https://doi.org/10.1039/D1CC05009E
[69] A. Gomez-Lopez, N. Ayensa, B. Grignard, L. Irusta, I. Calvo, A.J. Müller, C. Detrembleur, H. Sardon, Enhanced and reusable poly(hydroxy urethane)-based low temperature hot-melt adhesives, ACS Polym. Au. (2022). https://doi.org/10.1021/acspolymersau.1c00053
[70] D.J. Fortman, J.P. Brutman, C.J. Cramer, M.A. Hillmyer, W.R. Dichtel, Mechanically activated, catalyst-free polyhydroxyurethane vitrimers, J. Am. Chem. Soc. 137 (2015) 14019–14022. https://doi.org/10.1021/jacs.5b08084
[71] S. Hu, X. Chen, J.M. Torkelson, Biobased reprocessable polyhydroxyurethane networks: full recovery of crosslink density with three concurrent dynamic chemistries, ACS Sustain. Chem. Eng. 7 (2019) 10025–10034. https://doi.org/10.1021/acssuschemeng.9b01239
[72] X. Chen, L. Li, T. Wei, D.C. Venerus, J.M. Torkelson, Reprocessable polyhydroxyurethane network composites: effect of filler surface functionality on cross-link density recovery and stress relaxation, ACS Appl. Mater. Interfaces. 11 (2019) 2398–2407.
https://doi.org/10.1021/acsami.8b19100
[73] H. Blattmann, R. Mülhaupt, Multifunctional POSS cyclic carbonates and non-isocyanate polyhydroxyurethane hybrid materials, Macromolecules 49 (2016) 742–751.
https://doi.org/10.1021/acs.macromol.5b02560
[74] B. Zhao, K. Wei, L. Wang, S. Zheng, Poly(hydroxyl urethane)s with double decker silsesquioxanes in the main chains: synthesis, shape recovery, and reprocessing properties, Macromolecules 53 (2020) 434–444. https://doi.org/10.1021/acs.macromol.9b01976

[75] W. Liu, G. Hang, H. Mei, L. Li, and S. Zheng, Nanocomposites of polyhydroxyurethane with POSS microdomains: synthesis via non-isocyanate approach, morphologies and reprocessing properties. Polymers 14 (2022) 1331. https://doi.org/10.3390/polym14071331
[76] P. J. Flory, Principles of Polymer Chemistry, Cornell University Press, Ithaca, United States, 1953.
[77] A. Bossion, R.H. Aguirresarobe, L. Irusta, D. Taton, H. Cramail, E. Grau, D. Mecerreyes, C. Su, G. Liu, A.J. Müller, H. Sardon, Unexpected synthesis of segmented poly(hydroxyurea–urethane)s from dicyclic carbonates and diamines by organocatalysis, Macromolecules 51 (2018) 5556–5566. https://doi.org/10.1021/acs.macromol.8b00731
[78] K. Fancey, A mechanical model for creep, recovery and stress relaxation in polymeric materials, J. Mater. Sci. 40 (2005) 4827–4831. https://doi.org/10.1007/s10853-005-2020-x
[79] J.C. Hooker, J.M. Torkelson, Coupling of probe reorientation dynamics and rotor motions to polymer relaxation as sensed by second harmonic generation and fluorescence, Macromolecules 28 (1995) 7683–7692. https://doi.org/10.1021/ma00127a014
[80] D.J. Fortman, R.L. Snyder, D.T. Sheppard, W.R. Dichtel, Rapidly reprocessable cross-linked polyhydroxyurethanes based on disulfide exchange, ACS Macro Lett. 7 (2018) 1226–1231. https://doi.org/10.1021/acsmacrolett.8b00667
[81] L. H. Sperling, Introduction to Physical Polymer Science, John Wiley & Sons, Hoboken, United States, 2006.
[82] L.E. Nielsen, Cross-linking–effect on physical properties of polymers, J. Macromol. Sci., Part C 3 (1969) 69–103. https://doi.org/10.1080/15583726908545897
[83] D.J. Plazek, Effect of crosslink density on the creep behavior of natural rubber vulcanizates, J. Polym. Sci., Part A-2: Polym. Phys. 4 (1966) 745–763. https://doi.org/10.1002/pol.1966.160040507
[84] K. Watanabe, Stress relaxation and creep of several vulcanized elastomers, Rubber Chem. Technol. 35 (1962) 182–199. https://doi.org/10.5254/1.3539889
[85] M. Capelot, M.M. Unterlass, F. Tournilhac, L. Leibler, Catalytic control of the vitrimer

glass transition, ACS Macro Lett. 1 (2012) 789–792. https://doi.org/10.1021/mz300239f
[86] Y. Lu, Z. Guan, Olefin metathesis for effective polymer healing via dynamic exchange of strong carbon–carbon double bonds, J. Am. Chem. Soc. 134 (2012) 14226–14231. https://doi.org/10.1021/ja306287s
[87] W. Liu, D.F. Schmidt, E. Reynaud, Catalyst selection, creep, and stress relaxation in high-performance epoxy vitrimers, Ind. Eng. Chem. Res. 56 (2017) 2667–2672. https://doi.org/10.1021/acs.iecr.6b03829
[88] F. Snijkers, R. Pasquino, A. Maffezzoli, Curing and viscoelasticity of vitrimers, Soft Matter. 13 (2017) 258–268. https://doi.org/10.1039/C6SM00707D
[89] Y. Liu, Z. Tang, D. Wang, S. Wu, B. Guo, Biomimetic design of elastomeric vitrimers with unparalleled mechanical properties, improved creep resistance and retained malleability by metal–ligand coordination, J. Mater. Chem. A. 7 (2019) 26867–26876. https://doi.org/10.1039/C9TA10909A

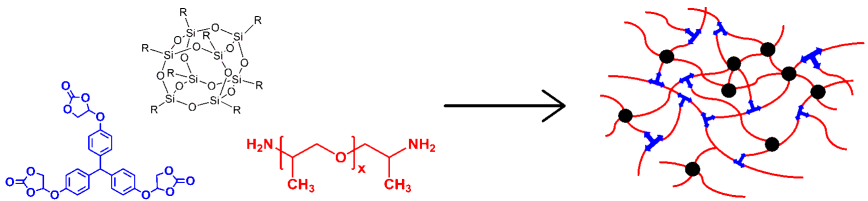

Reprocessable PHU-POSS network composite

Conventional Silica Nanoparticles

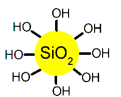

Property loss after reprocessing

Reactive POSS

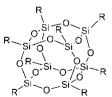

Full property recovery after reprocessing